Bone Microarchitecture and Strength Adaptation to Physical Activity:

A Within-Subject Controlled, HRpQCT Study

Stuart J. Warden[1,2,3], Christian S. Wright[1,2] and Robyn K. Fuchs[1,2]

[1]Department of Physical Therapy, School of Health and Human Sciences, Indiana University, Indianapolis, IN; [2]Indiana Center for Musculoskeletal Health, Indiana University, Indianapolis, IN; [3]La Trobe Sport and Exercise Medicine Research Centre, La Trobe University, Bundoora, Victoria, Australia

Send correspondence to: Stuart J. Warden, Department of Physical Therapy, School of Health & Human Sciences, Indiana University, 1140 W. Michigan St., CF-124, Indianapolis, IN 46202 (stwarden@iu.edu)

_____

ABSTRACT

Purpose: Physical activity benefits bone mass and cortical bone size. The current study assessed the impact of chronic (≥10 years) physical activity on trabecular microarchitectural properties and micro-finite element (µFE) analyses of estimated bone strength. **Methods:** Female collegiate-level tennis players (n=15; age=20.3±0.9 yrs) were used as a within-subject controlled model of chronic unilateral upper-extremity physical activity. Racquet-to-nonracquet arm differences at the distal radius and radial diaphysis were assessed using high-resolution peripheral computed tomography (HRpQCT). The distal tibia and tibial diaphysis in both legs were also assessed, and cross-country runners (n=15; age=20.8±1.2 yrs) included as controls. **Results:** The distal radius of the racquet arm had 11.8% (95% confidence interval [CI], 7.9 to 15.7%) greater trabecular bone volume/tissue volume, with trabeculae that were greater in number, thickness, connectivity, and proximity to each other than in the nonracquet arm (all p<0.01). Combined with enhanced cortical bone properties, the microarchitectural advantages at the distal radius contributed a 18.7% (95% CI, 13.0 to 24.4%) racquet-to-nonracquet arm difference in predicted load before failure. At the radial diaphysis, predicted load to failure was 9.6% (95% CI, 6.7 to 12.6%) greater in the racquet vs. nonracquet arm. There were fewer and smaller side-to-side differences at the distal tibia; however, the tibial diaphysis in the leg opposite the racquet arm was larger with a thicker cortex and had 4.4% (95% CI, 1.7 to 7.1%) greater strength than the contralateral leg. **Conclusion:** Chronically elevated physical activity enhances trabecular microarchitecture and µFE estimated strength, furthering observations from short-term longitudinal studies. The data also demonstrate tennis players exhibit crossed symmetry wherein the leg opposite the racquet arm possesses enhanced tibial properties

compared to in the contralateral leg. **Keywords:** distal radius, exercise, finite element, HRpQCT,

mechanoadaptation, osteoporosis

INTRODUCTION

Bone strength and the ability to resist fracture is determined by the amount and quality of bone material present and its organization. These properties are largely genetically determined, but mechanoadaptation plays an important role. For instance, the humeral diaphysis in professional baseball players would fracture during a single pitch if adaptation to throwing-related forces had not increased bone mass and size to double bone strength (1).

A wealth of studies have demonstrated skeletal adaptation to loads associated with physical activity (2). Benefits have principally been demonstrated using dual-energy x-ray absorptiometry (DXA) and low-resolution (voxel size ≥200 µm) peripheral quantitative computed tomography (pQCT). The projectional 2D bone mass measures provided by DXA are influenced by size-artifacts and do not adequately assess bone structural or compartmental adaptation (3). pQCT can assess bone size and isolated cortical and trabecular compartment adaptation, but its low spatial resolution contributes to partial volume effects and an inability to resolve trabecular microarchitecture (3, 4).

There is a need to explore the impact of physical activity on trabecular microarchitecture. Microarchitecture contributes to overall bone strength independent of bone density, with a loss of trabecular connectivity producing a disproportionate loss of strength (5). With the advent of high-resolution pQCT (HRpQCT) it is now possible to assess bone microarchitectural properties as well as use micro-finite element (µFE) analyses to estimate bone strength (6). Bone strength estimates from HRpQCT data predict incident fracture and improve fracture prediction beyond

femoral neck areal bone mineral density (BMD) or fracture risk assessment tool (FRAX) scores alone (7, 8).

There are a limited, but growing, number of studies reporting the benefits of physical activity on HRpQCT measures of bone microarchitecture and strength (9-17). Cross-sectional studies report enhanced microarchitecture and strength in those with greater participation in bone-centric physical activities (9, 12-14, 16, 17), but comparing physical activity effects between individuals may be confounded by between-individual differences in inherited traits and systemic factors. Longitudinal studies have reported enhanced bone microarchitecture and strength development with increasing levels of moderate-to-vigorous physical activity during adolescence (10), and changes in microarchitecture and strength in as little as 8-13 weeks of arduous military training (11, 15). However, longitudinal studies performed to date have not explored the impact of elevated physical activity performed over prolonged period on HRpQCT measures of bone microarchitecture and strength.

Within-subject controlled study designs assessing side-to-side differences (i.e., asymmetry) in individuals who have preferentially exercised one side of their body are effective and efficient at exploring the skeletal benefit of chronically elevated physical activity. Compared to in studies comparing between individuals, individuals in within-subject controlled studies serve as their own controls to minimize the impact of inherited traits and systemic factors. The most well-known within-subject controlled model is tennis players (18). Previous studies have compared the racquet and non-racquet arms in tennis players to demonstrate benefits on cortical bone mass and size and trabecular bone mass (19-23). To our knowledge, no study has explored

the impact of a prolonged history of racquet sport playing on HRpQCT measures of bone microarchitecture and strength.

The aim of the current study was to explore the impact of chronically ($\geq$10 years) elevated unilateral physical activity on HRpQCT measures of bone microarchitecture and strength of the radius by comparing the racquet and non-racquet arms of collegiate-level tennis players. Sites of interest included the distal radius and radial diaphysis, and it was hypothesized the racquet would have enhanced bone microarchitecture and strength at both sites. Athletic control subjects (collegiate-level cross-country runners) were tested to explore whether asymmetry observed in tennis players was due to simple arm dominance. We also assessed HRpQCT measures of bone microarchitecture and strength in the distal tibia and tibial diaphysis as it was hypothesized the lower extremity opposite the racquet arm in tennis players would possess enhanced properties due to the phenomenon of crossed symmetry (24, 25).

METHODS

Study design and participants

A within-subject controlled cross-sectional study design was used to compare the dominant and nondominant radius and tibia in female tennis players and cross-country runners. Eligible subjects were current members of a tennis or cross-country team competing at the Division I, II or III level within the National Collegiate Athletic Association. Tennis players must have started playing competitive tennis at least 3 years prior to their self-reported age of menarche, played for a minimum of 10 years, and reported using a single-handed forehand technique. Cross-country runners were included if they did not have a history of participating

more than twice per month for >6 months in an activity that may expose the upper or lower extremities to asymmetrical loading (e.g. racquet sports, soccer, ten-pin bowling, baseball, softball, etc.). Exclusion criteria were: 1) known metabolic bone disease; 2) history of a radial or tibial fracture or stress fracture within the past 2 years; 3) implanted metal within any of the HR-pQCT scan sites; 4) exposure to upper or lower extremity immobilization for more than 2 weeks within the past 2 years, and; 5) self-reported menstrual dysfunction. Arm dominance was defined as the athlete's racquet arm (tennis) or preferred throwing arm (runners). Leg dominance was defined as the leg contralateral to the dominant arm. The study was approved by the Institutional Review Board of Indiana University and written informed consent was obtained from all participants.

Dual-energy x-ray absorptiometry (DXA)

DXA (Norland Elite; Norland at Swissray, Fort Atkinson, WI) was used to assess whole-body composition. The manufacturer's standard scan and positioning protocols were used. Short-term precision on repeat scans following repositioning in 15 individuals showed root mean square coefficients of variation (RMS-CVs) of <1%, 1.2%, and 3.0% for whole-body bone mineral density, lean mass, and fat mass, respectively.

High-resolution peripheral quantitative computed tomography (HRpQCT).

HRpQCT (XtremeCT II; Scanco Medical, Bruttisellen, Switzerland) was used to acquire three-dimensional bone macro- and microarchitecture, and volumetric bone mineral density (vBMD) at the bilateral distal and diaphyseal radius and tibia. The scanner operated at 68 kVp and 1.47 mA to acquire 168 slices (10.2 mm of bone length) with a voxel size of 60.7 µm. After

performance of a scout view, reference lines were placed at the medial edge of the distal radius and center of the tibia joint surface. Scan stacks were centered 4% and 30% of bone length proximal to the radius reference line, and 7.3% and 30% of bone length proximal to the tibia reference line. Bone length was measured using anthropometric calipers. Percent offsets were used to enable assessment of anatomically similar regions (26). Scans were scored for motion artifacts on a standard scale of 1 (no motion) to 5 (significant blurring of the periosteal surface, discontinuities in the cortical shell) (27). Scans scoring ≥3 were repeated up to 2 times.

Reconstructed images were analyzed according to the manufacturer's standard protocol. The outer periosteal and inner endosteal surfaces of the bone were identified automatically, and segmentations checked for accuracy and manually modified when needed. To assess microarchitectural outcomes, images were filtered using a low-pass Gaussian filter (sigma 0.8, support 1.0) and fixed thresholds used to extract trabecular and cortical bone (320 and 450 mgHA/cm^3, respectively). The following outcomes were recorded at distal metaphyseal sites: total vBMD (Tt.vBMD, mgHA/cm^3) and area (Tt.Ar, mm^2); trabecular vBMD (Tb.vBMD, mgHA/cm^3), area (Tb.Ar, mm^2), bone volume/total volume (Tb.BV/TV, %), thickness (Tb.Th, µm), number (Tb.N, 1/mm), separation (Tb.Sp, µm), and connectivity density (Conn.D, 1/mm^3), and; cortical vBMD (Ct.vBMD, mgHA/cm^3), area (Ct.Ar, mm^2), thickness (Ct.Th, mm). The following outcomes were measured at diaphyseal sites: total area (Tt.Ar, mm^2); and cortical tissue mineral density (Ct.TMD, mgHA/cm^3), vBMD (Ct.vBMD, mgHA/cm^3), area (Ct.Ar, mm^2), thickness (Ct.Th, mm), and porosity (Ct.Po, %).

μFE analysis (Scanco Medical FE software version 1.13) was used to estimate stiffness (kN/mm) and failure load (kN) at both the metaphyseal and diaphyseal sites. In brief, each voxel was assigned a modulus of 10 GPa and Poisson's ratio of 0.3 (28). Uniaxial compression was applied and failure load estimated when 2% of the elements exceeded 0.7% strain (28). The μFE model has been validated to estimate bone mechanical properties within both the radius and tibia (29).

Short-term precision on repeat scans following repositioning in 15 individuals showed RMS-CVs of <0.5% for bone density and 0.3-1.1% for cortical and trabecular areal and thickness measures at the diaphyseal and metaphyseal sites; 0.7-1.1% for BV/TV at the metaphyseal sites, and; <1% and 1.8-2.9% for stiffness and failure load at the diaphyseal and metaphyseal sites, respectively.

Statistical analyses

Two-tailed analyses with α = 0.05 were performed with IBM SPSS Statistics (v25; SPSS Inc., Chicago, IL). Demographic and anthropometric characteristics, and bone properties in the nondominant (ND) limbs were compared between groups using unpaired t-tests. Side-to-side differences between the dominant (D) and ND limbs were assessed by calculating mean absolute (D–ND) and mean percent ([D–ND]/ND x 100%) differences and their 95% confidence intervals (CI). Mean absolute and percent differences were assessed by single sample t-tests with a population mean of 0. D-to-ND percent differences were compared between groups using unpaired t-tests.

RESULTS

Participant characteristics

Tennis players and runners were comparable in age, self-reported age of menarche, height, areal bone mineral density, and lean mass (all p=0.08-0.57) (Table 1). Tennis players were 21% heavier than runners, and had a higher BMI and fat mass (all p<0.01). There were no group differences in HRpQCT measures of the ND extremities at the distal radius (all p=0.11-0.81; see Table, Supplemental Digital Content, 1 HR-pQCT properties of the distal radius in runners and tennis players, http://links.lww.com/MSS/C213), radial diaphysis (all p=0.50-0.98; see Table, Supplemental Digital Content 2, HR-pQCT properties of the radial diaphysis in runners and tennis players, http://links.lww.com/MSS/C214) or tibial diaphysis (all p=0.14-0.81; see Table, Supplemental Digital Content 3, HR-pQCT properties of the tibial diaphysis in runners and tennis players, http://links.lww.com/MSS/C215). Tennis players had 11% greater Tt.Ar at the distal tibia in the ND leg compared to runners (p<0.05; see Table, Supplemental Digital Content 4, HR-pQCT properties of the distal tibia in runners and tennis players, http://links.lww.com/MSS/C216). There were no other group differences in HRpQCT measures at the distal tibia of the ND leg (all p=0.07-0.78).

Distal radius

There were no D-to-ND arm differences in distal radius density, size, microarchitecture, or strength in runners (all p=0.26 to 0.78; Fig. 1A; and Supplemental Digital Content, 1 HR-pQCT properties of the distal radius in runners and tennis players, http://links.lww.com/MSS/C213). Representative reconstructed HRpQCT images of the distal radius in a tennis player are shown in Figure 2A. Tennis players had 8.3% (95% CI, 2.8 to

13.8%) greater Tt.vBMD in their D arm compared to ND arm, with 10.9% (95% CI, 6.5 to 15.3%) greater Tb.vBMD ($p<0.001$), but not Ct.vBMD ($p=0.97$) (Fig. 1A). The distal radius in the D arm of tennis players was 6.8% (95% CI, 3.4 to 10.2%) larger than in the ND arm, with enhanced D-to-ND arm differences in Ct.Ar, Tb.Ar, and Ct.Th (all $p<0.03$) (Fig. 1A and 2B). The trabecular compartment of the distal radius in tennis players had a D-to-ND arm difference of 11.8% (95% CI, 7.9 to 15.7%) in Tb.BV/TV, with the D arm having thicker (Tb.Th; Fig. 2C) and more (Tb.N) trabeculae that were closer (Tb.Sp) and more connected (Conn.D) than in the ND arm (all $p<0.01$) (Fig. 1A). The density, size, and microarchitectural D-to-ND arm differences in tennis players cumulated in 18.7% (95% CI, 13.0 to 24.4%) and 20.0% (95% CI, 13.8 to 26.2%) D-to-ND arm differences in distal radius failure load and stiffness, respectively (Fig. 1A). The D-to-ND differences in tennis players at the distal radius for density (Tt.vBMD, Tb.vBMD), size (Tt.Ar, Ct.Ar), microarchitecture (Ct.Th, Tb.BV/TV, Tb.Th, Tb.N, Tb.Sp, Conn.D), and strength (failure load, stiffness) differed from D-to-ND differences in runners (all $p<0.05$; Fig. 1A).

Radial diaphysis

Runners had 0.3% (95% CI, 0.1 to 0.4%) greater Ct.vBMD and Ct.TMD at the radial diaphysis in their D arm relative to ND arm ($p=0.02$; Fig. 1B; and Supplemental Digital Content 2, HR-pQCT properties of the radial diaphysis in runners and tennis players, http://links.lww.com/MSS/C214). There were no other D-to-ND arm differences in radial diaphysis density, size, microarchitecture, or strength in runners (all $p=0.14$ to 0.94) (Fig. 1B). Representative reconstructed HRpQCT images of the radial diaphysis in a tennis player are shown in Figure 3A. Tennis players had 0.3% (95% CI, 0.1 to 0.5%) lower Ct.vBMD and

Ct.TMD at the radial diaphysis in their D arm relative to ND arm (p=0.02) (Fig. 1B). The radial diaphysis in the D arm of tennis players was larger (Tt.Ar and Ct.Ar) and had a thicker cortex (Ct.Th; Fig. 3B) compared to the ND-arm (all p<0.01), but there were no D-to-ND arm differences in Ct.Po (p=0.71) (Fig. 1B). The density, size, and microarchitectural D-to-ND arm differences in tennis players contributed to D-to-ND arm differences of 9.6% (95% CI, 6.7 to 12.6%) and 10.3% (95% CI, 7.2 to 13.4%) D-to-ND arm for radial diaphysis failure load and stiffness, respectively (Fig. 1B). The D-to-ND differences in tennis players at the radial diaphysis for all measures differed from D-to-ND differences in runners (all p<0.01), except for Ct.Po (p=0.75) (Fig. 1B).

Distal tibia

There were no D-to-ND arm differences in distal tibia density, size, microarchitecture, or strength in runners (all p=0.07 to 0.87; Fig. 1C; and Supplemental Digital Content 4, HR-pQCT properties of the distal tibia in runners and tennis players, http://links.lww.com/MSS/C216). Representative reconstructed HRpQCT images of the distal radius in a tennis player are shown in Figure 4A. Tennis players had D-to-ND leg differences in Tt.vBMD, failure load, and stiffness at the distal tibia (all p<0.05) (Fig. 1C). For each of these three variables, the D-to-ND differences in tennis players did not differ from D-to-ND differences in runners (all p=0.22 to 0.77) (Fig. 1C).

Tibial diaphysis

Runners had no D-to-ND leg differences at the tibial diaphysis for any HR-pQCT measure (all p=0.07 to 0.52; Fig. 1D; and Supplemental Digital Content 3, HR-pQCT properties

of the tibial diaphysis in runners and tennis players, http://links.lww.com/MSS/C215).

Representative reconstructed HRpQCT images of the tibial diaphysis in a tennis player are

shown in Figure 5A. There were no D-to-ND differences in Ct.vBMD, Ct.TMD or Ct.Po at the

tibial diaphysis in tennis players (all p=0.32 to 0.74). Tennis players had a 2.2% (95% CI, 0.5 to

3.9%) D-to-ND difference in tibial diaphysis Tt.Ar, with D-to-ND differences in Ct.Ar and Ct.Th

(all p<0.05) (Fig. 1D and 5B). The tibial diaphysis in the D leg of tennis players had 4.4% (95%

CI, 1.7 to 7.1%) and 4.6% (95% CI, 2.0 to 7.3%) greater failure load and stiffness compared to

the ND leg, respectively (Fig. 1D). The D-to-ND differences in tennis players at the tibial

diaphysis differed from D-to-ND differences in runners (all p≤0.03), except for Ct.vBMD,

Ct.TMD, Ct.Po (all p=0.53 to 0.81) (Fig. 1D).

DISCUSSION

The current data are novel as they demonstrate the impact of chronically (≥10 years)

elevated physical activity (i.e. mechanical loading) on bone microarchitecture and µFE estimated

strength. Using female tennis players as an established within-subject controlled model of

unilateral physical activity, we detected greater bone mass (13.8% [95% CI, 9.8-17.9%];

calculated from Tt.vBMD x Tt.Ar) and size (Tt.Ar) at the distal radius in the racquet arm

compared to nonracquet arm. These observations confirm previous studies utilizing low-

resolution pQCT (voxel size = 500-590 µm) (19, 21-23, 30); however, our use of HRpQCT with

8-10 times greater resolution (voxel size = 60.7 µm) enabled us to also reveal the distal radius in

the racquet arm had more trabeculae (Tb.N) which were thicker (Tb.Th), closer together (Tb.Sp),

and more connected (Conn.D) than in the nonracquet arm. The side-to-side differences in

trabecular microarchitecture were not due to asymmetrical habitual loading associated with simple limb dominance, as tennis players had larger dominant-to-nondominant arm differences than athletic controls (cross-country runners). The cumulative differences in bone mass, size, and microarchitecture between the racquet and nonracquet arms in tennis players contributed to the distal radius in the racquet arms having 18.7% (95% CI, 13.0 to 24.4%) greater strength (failure load) to simulated uniaxial compressive loading, as determined using µFE analysis.

Our data expand on those of recent longitudinal studies by showing the impact of chronically elevated physical activity on bone microarchitecture and µFE estimated strength. Hughes et al. (11) demonstrated the utility of HRpQCT in detecting acute physical activity-related bone changes within 8 weeks—a shorter time frame than previously able using either DXA or low-resolution pQCT. They detected changes of 1-2% in microarchitectural (Ct.Th, Tb.BV/TV, Tb.Th, Tb.N) and 2.5% in strength outcomes at the distal tibia in female recruits undergoing basic combat training. Similarly, O'Leary et al. (15) observed improvements Tb.BV/TV and Ct.Th at the distal tibia in male infantry recruits over 13 weeks of basic training. The latter study did not detect changes in Tb.Th or Tb.N, despite a longer study period than Hughes et al. (11). This may have been due to O'Leary et al.'s (15) use of a first generation HRpQCT which has a resolution (voxel size = 82 µm) at the limit to accurately determine the thickness of individual trabeculae. Neither Hughes et al. (11) or O'Leary et al. (15) studied physical activity effects on the distal radius, the most common site for fracture in both adults and children (32, 33). It would be interesting for future studies to explore whether our observed benefits in trabecular microarchitecture persist long-term, as suggested by a previous preclinical study (34), and whether there are persisting benefits on estimated bone strength.

We also studied the radial diaphysis, distal tibia, and tibial diaphysis. Tennis players had expected changes at the radial diaphysis, 30% proximal from the distal end of the bone. Changes included reduced density (Ct.vBMD) and enlarged size (Tt.Ar, Ct.Ar, and Ct.Th) of the cortical compartment. A reduction in cortical density with physical activity is established (1, 11, 35), yet the mechanism remains to be elucidated. It may be due to a combination of modeling-related new bone on the periosteal and endosteal surfaces being less mineralized or the presence of a greater volume of targeted intracortical remodeling (36). The latter may cause increased intracortical porosity and/or greater volumes of younger, less mineralized bone tissue. HRpQCT has the potential to reveal cortical porosity; however, the threshold-based approach utilized by the XtremeCT analysis software is unable to capture pores with diameters below the spatial resolution of the scanner resulting in an underestimation of porosity by 3 to 11% (37). Because of the very low porosity (<0.5%) detected in our population of young adults and poor short-term precision of its assessment (RMS-CVs = 5-7%), there were very wide confidence intervals (±20% between sides) and no side-to-side or between group differences observed in our dataset.

Any impact altered Ct.vBMD had on bone strength at the radial diaphysis within the racquet arm was overshadowed by greater cortical bone mass (9.3% [95% CI, 6.7-11.9%]; calculated from Ct.vBMD x Ct.Ar) and size. Using the μFE computer modeling approach, racquet arms had ~10% greater strength (failure load) to simulated axial loading at the radial diaphysis. Some of this strength benefit at this cortical-rich site is anticipated to persist lifelong even after cessation of tennis (i.e. unilateral physical activity) (1, 38). However, unlike at the distal radius, μFE models for estimating strength within the radial diaphysis have not been validated using experimental loading tests of cadaveric bones.

Another novel finding in the current study was the observation of enhanced tibial properties in the dominant leg in tennis players. The dominant leg was defined as the leg opposite the racquet arm, and was predicted to have enhanced properties due to crossed symmetry (24, 25). Crossed symmetry in tennis players may occur due to the leg opposite the racquet arm being used to generate forces that are transmitted across the body from the leg and trunk to the racquet arm during forehand strokes, and due to the braking (and subsequent push-off) forces experienced when serving and volleying (39-41). There is limited evidence of musculoskeletal crossed symmetry in tennis players. Previous studies have reported no lower extremity asymmetry in bone mass (assessed using DXA) (42) or muscle strength (43, 44) in junior tennis players, or calculated asymmetry as the difference between the leg with higher versus lower measures (45, 46) and not according to limb dominance. However, male tennis players have previously been reported to have greater iliopsoas and gluteal muscle size and whole-leg bone mass on the side opposite their racquet arm (42, 47).

The current study did not observe differences in background bone properties between the tennis players and cross-country runners. The two groups of athletes had comparable properties on whole-body DXA and HRpQCT assessment of their nondominant extremities. This was unexpected as tennis activities are thought to introduce more multidirectional loads with higher impacts than distance running to induce greater adaptation and enhance bone health (48, 49). The absence of group differences in the current study may relate to the relatively good health of the cross-country athletes we recruited, who all had a BMI >19 kg/m^2 and normal menstrual function, and the comparable lean mass between groups, with all the cross-country athletes reporting regular performance of high-load resistance training.

Our study had a number of strengths, including the: 1) use of a within-subject controlled model to address selection bias; 2) inclusion of a comparable athletic control group to account for crossed symmetry due to elevated habitual unilateral loading associated with simple limb dominance, and; 3) use of HRpQCT to provide measures of bone microarchitecture and µFE-estimated strength. However, the study also possesses a number of limitations, including the non-study of males and potential for partial volume effects, particularly when assessing small structures such as trabeculae and the cortical shell at the distal radius and tibia.

In summary, the current study demonstrated the impact of chronically (≥10 years) elevated physical activity on bone microarchitecture and µFE estimated strength in females using a within-subject controlled model. Enhancements in bone mass, size, and microarchitecture at the distal radius in the racquet arm of tennis players endowed the bone with nearly 20% greater strength to axial compressive loading than in the contralateral nonracquet arm. Because of crossed symmetry, the tibia in the leg opposite the racket arm had enhanced bone properties compared to the contralateral leg. These observations extend recent findings of the benefit of acute physical activity on bone microarchitecture and µFE estimated strength outcomes.

ACKNOWLEDGEMENTS

Author contributions statement: S.J.W. and R.K.F. contributed to study design; all authors contributed to the acquisition, analysis and interpretation of data; S.J.W. drafted the paper; all authors critically revised the paper and approve of its final version.

REFERENCES

1. Warden SJ, Mantila Roosa SM, Kersh ME, et al. Physical activity when young provides lifelong benefits to cortical bone size and strength in men. Proc Natl Acad Sci U S A. 2014;111:5337-42.

2. Cauley JA, Giangregorio L. Physical activity and skeletal health in adults. Lancet Diabetes Endocrinol. 2020;8(2):150-62.

3. Adams JE. Advances in bone imaging for osteoporosis. Nat Rev Endocrinol. 2013;9(1):28-42.

4. Prevrhal S, Engelke K, Kalender WA. Accuracy limits for the determination of cortical width and density: the influence of object size and CT imaging parameters. Phys Med Biol. 1999;44(3):751-64.

5. Parfitt AM. Trabecular bone architecture in the pathogenesis and prevention of fracture. Amercian Journal of Medicine. 1987;82:S68-S72.

6. Whittier DE, Boyd SK, Burghardt AJ, et al. Guidelines for the assessment of bone density and microarchitecture in vivo using high-resolution peripheral quantitative computed tomography. Osteoporos Int. 2020;31(9):1607-27.

7. Mikolajewicz N, Bishop N, Burghardt AJ, et al. HR-pQCT Measures of Bone Microarchitecture Predict Fracture: Systematic Review and Meta-Analysis. J Bone Miner Res. 2020;35(3):446-59.

8. Samelson EJ, Broe KE, Xu H, et al. Cortical and trabecular bone microarchitecture as an independent predictor of incident fracture risk in older women and men in the Bone

Microarchitecture International Consortium (BoMIC): a prospective study. Lancet Diabetes Endocrinol. 2019;7(1):34-43.

9. Burt LA, Schipilow JD, Boyd SK. Competitive trampolining influences trabecular bone structure, bone size, and bone strength. J Sport Health Sci. 2016;5(4):469-75.

10. Gabel L, Macdonald HM, Nettlefold L, McKay HA. Physical activity, sedentary time, and bone strength from childhood to early adulthood: a mixed longitudinal HR-pQCT study. J Bone Miner Res. 2017;32:1525-36.

11. Hughes JM, Gaffney-Stomberg E, Guerriere KI, et al. Changes in tibial bone microarchitecture in female recruits in response to 8 weeks of U.S. Army Basic Combat Training. Bone. 2018;113:9-16.

12. Langsetmo L, Burghardt AJ, Schousboe JT, et al. Objective measures of moderate to vigorous physical activity are associated with higher distal limb bone strength among elderly men. Bone. 2020;132:115-198.

13. McKay H, Liu D, Egeli D, Boyd S, Burrows M. Physical activity positively predicts bone architecture and bone strength in adolescent males and females. Acta Paediatr. 2011;100(1):97-101.

14. Ng CA, McMillan LB, Beck B, Humbert L, Ebeling PR, Scott D. Associations between physical activity and bone structure in older adults: does the use of self-reported versus objective assessments of physical activity influence the relationship? Osteoporos Int. 2020;31(3):493-503.

15.   O'Leary TJ, Izard RM, Walsh NP, Tang JCY, Fraser WD, Greeves JP. Skeletal macro- and microstructure adaptations in men undergoing arduous military training. Bone. 2019;125:54-60.

16.   Popp KL, Turkington V, Hughes JM, et al. Skeletal loading score is associated with bone microarchitecture in young adults. Bone. 2019;127:360-6.

17.   Schipilow JD, Macdonald HM, Liphardt AM, Kan M, Boyd SK. Bone micro-architecture, estimated bone strength, and the muscle-bone interaction in elite athletes: an HR-pQCT study. Bone. 2013;56(2):281-9.

18.   Jones H, Priest J, Hayes W, Tichenor C, Nagel D. Humeral hypertrophy in response to exercise. J Bone Joint Surg. 1977;59A(2):204-7.

19.   Ashizawa N, Nonaka K, Michikami S, et al. Tomographical description of tennis-loaded radius: reciprocal relation between bone size and volumetric BMD. J Appl Physiol. 1999;86(4):1347-51.

20.   Haapasalo H, Kannus P, Sievänen H, et al. Effect of long term unilateral activity on bone mineral density of female junior tennis players. J Bone Miner Res. 1998;13:310-9.

21.   Ireland A, Maden-Wilkinson T, Ganse B, Degens H, Rittweger J. Effects of age and starting age upon side asymmetry in the arms of veteran tennis players: a cross-sectional study. Osteoporos Int. 2014;25(4):1389-400.

22.   Ireland A, Maden-Wilkinson T, McPhee J, et al. Upper limb muscle-bone asymmetries and bone adaptation in elite youth tennis players. Med Sci Sports Exerc. 2013;45(9):1749-58.

23. Kontulainen S, Sievanen H, Kannus P, Pasanen M, Vuori I. Effect of long-term impact-loading on mass, size, and estimated strength of humerus and radius of female racquet-sports players: a peripheral quantitative computed tomography study between young and old starters and controls. J Bone Miner Res. 2003;18(2):352-9.

24. Auerbach BM, Ruff CB. Limb bone bilateral asymmetry: variability and commonality among modern humans. J Hum Evol. 2006;50(2):203-18.

25. Peters M. Footedness: asymmetries in foot preference and skill and neuropsychological assessment of foot movement. Psychol Bull. 1988;103(2):179-92.

26. Shanbhogue VV, Hansen S, Halekoh U, Brixen K. Use of Relative vs Fixed Offset Distance to Define Region of Interest at the Distal Radius and Tibia in High-Resolution Peripheral Quantitative Computed Tomography. J Clin Densitom. 2015;18(2):217-25.

27. Sode M, Burghardt AJ, Pialat JB, Link TM, Majumdar S. Quantitative characterization of subject motion in HR-pQCT images of the distal radius and tibia. Bone. 2011;48(6):1291-7.

28. Pistoia W, van Rietbergen B, Lochmuller EM, Lill CA, Eckstein F, Ruegsegger P. Estimation of distal radius failure load with micro-finite element analysis models based on three-dimensional peripheral quantitative computed tomography images. Bone. 2002;30(6):842-8.

29. Zhou B, Wang J, Yu YE, et al. High-resolution peripheral quantitative computed tomography (HR-pQCT) can assess microstructural and biomechanical properties of both human distal radius and tibia: Ex vivo computational and experimental validations. Bone. 2016;86:58-67.

30.   Haapasalo H, Kontulainen S, Sievanen H, Kannus P, Jarvinen M, Vuori I. Exercise-induced bone gain is due to enlargement in bone size without a change in volumetric bone density: a peripheral quantitative computed tomography study of the upper arms of male tennis players. Bone. 2000;27(3):351-7.

31.   Kemp TD, de Bakker CMJ, Gabel L, et al. Longitudinal bone microarchitectural changes are best detected using image registration. Osteoporos Int. 2020; 31(10):1995-2005.

32.   Court-Brown CM, Caesar B. Epidemiology of adult fractures: A review. Injury. 2006;37(8):691-7.

33.   Randsborg PH, Gulbrandsen P, Saltytė Benth J, et al. Fractures in children: epidemiology and activity-specific fracture rates. J Bone Joint Surg Am. 2013;95(7):e42.

34.   Warden SJ, Galley MR, Hurd AL, et al. Cortical and trabecular bone benefits of mechanical loading are maintained long-term in mice independent of ovariectomy. J Bone Miner Res. 2014;29:1131-40.

35.   Warden SJ, Bogenschutz ED, Smith HD, Gutierrez AR. Throwing induces substantial torsional adaptation within the midshaft humerus of male baseball players. Bone. 2009;45(5):931-41.

36.   Gocha TP, Agnew AM. Spatial variation in osteon population density at the human femoral midshaft: histomorphometric adaptations to habitual load environment. J Anat. 2016;228(5):733-45.

37.   Jorgenson BL, Buie HR, McErlain DD, Sandino C, Boyd SK. A comparison of methods for in vivo assessment of cortical porosity in the human appendicular skeleton. Bone. 2015;73:167-75.

38. Warden SJ, Galley MR, Hurd AL, et al. Elevated mechanical loading when young provides lifelong benefits to cortical bone properties in female rats independent of a surgically induced menopause. Endocrinology. 2013;154(9):3178-87.

39. Chow JW, Carlton LG, Chae WS, Shim JH, Lim YT, Kuenster AF. Movement characteristics of the tennis volley. Med Sci Sports Exerc. 1999;31(6):855-63.

40. Kovacs M, Ellenbecker T. An 8-stage model for evaluating the tennis serve: implications for performance enhancement and injury prevention. Sports health. 2011;3(6):504-13.

41. Reid M, Elliott B, Crespo M. Mechanics and learning practices associated with the tennis forehand: a review. Journal of sports science & medicine. 2013;12(2):225-31.

42. Palaiothodorou D, Antoniou T, Vagenas G. Bone asymmetries in the limbs of children tennis players: testing the combined effects of age, sex, training time, and maturity status. J Sports Sci. 2020; 38(20):2298-306.

43. Ellenbecker TS, Roetert EP. Concentric isokinetic quadricep and hamstring strength in elite junior tennis players. Isokinetics and Exercise Science. 1995;5:3-6.

44. Ellenbecker TS, Roetert EP, Sueyoshi T, Riewald S. A descriptive profile of age-specific knee extension flexion strength in elite junior tennis players. Br J Sports Med. 2007;41(11):728-32.

45. Madruga-Parera M, Romero-Rodríguez D, Bishop C, Beltran-Valls MR, Latinjak AT, Beato M, et al. Effects of maturation on lower limb neuromuscular asymmetries in elite youth tennis players. Sports (Basel). 2019;7(5):106.

46.   Sannicandro I, Cofano G, Rosa RA, Piccinno A. Balance training exercises decrease lower-limb strength asymmetry in young tennis players. Journal of sports science & medicine. 2014;13(2):397-402.

47.   Sanchis-Moysi J, Idoate F, Izquierdo M, Calbet JA, Dorado C. Iliopsoas and gluteal muscles are asymmetric in tennis players but not in soccer players. PLoS ONE. 2011;6(7):e22858.

48.   Nikander R, Sievanen H, Uusi-Rasi K, Heinonen A, Kannus P. Loading modalities and bone structures at nonweight-bearing upper extremity and weight-bearing lower extremity: a pQCT study of adult female athletes. Bone. 2006;39(4):886-94.

49.   Tenforde AS, Carlson JL, Sainani KL, et al. Sport and triad risk factors influence bone mineral density in collegiate athletes. Med Sci Sports Exerc. 2018;50(12):2536-43.

FIGURE LEGENDS

Figure 1. Effect of chronically elevated physical activity on HRpQCT acquired properties at the: **A)** distal radius; **B)** radial diaphysis; **C)** distal tibia, and; **D)** tibial diaphysis. Data represent the mean percent difference between the dominant and nondominant limbs in tennis players (closed circles) and runners (open circles). Error bars indicate 95% confidence intervals (CIs). * indicates 95% CIs that do not contain 0%, with 95% CIs to the right of 0% indicating greater values in the dominant limb. † indicates significant difference ($p<0.05$, unpaired t-test) between groups (tennis vs. control).

Figure 2. Reconstructed HRpQCT images showing: **A)** the whole bone; **B)** cortical thickness; **C)** trabecular thickness, and; **D)** von Mises stresses at the distal radius in the nondominant (ND) and dominant (D) arms of a representative tennis player. Note the 4.1% larger Tt.Ar (i.e. size) in the D arm of this participant (A), with 16.9% thicker cortex (B), and 5.9% thicker trabeculae (C). The thickened cortex and trabeculae are particularly evident on the anterior side of the D arm in this particular participant, who had D-to-ND arm differences of 11.3% and 29.7% for Tb.BV/TV and failure load, respectively.

Figure 3. Reconstructed HRpQCT images showing: **A)** the whole bone and **B)** cortical thickness at the radial diaphysis in the nondominant (ND) and dominant (D) arms of the representative tennis player shown in Figure 2. Note the larger Tt.Ar (i.e. size) in the dominant arm with bigger medullary cavity (D-to-ND arm difference in medullary area in tennis players = 22.8% [95% CI, 5.4-40.3], as calculated by Tt.Ar minus Ct.Ar). Despite a larger medullary area, the greater Tt.Ar in the dominant arm of tennis players resulted in greater Ct.Th. The tennis player shown had

21.3%, 15.7%, 1.9% and 16.4% D-to-ND arm differences in Tt.Ar, Ct.Ar, Ct.Th, and failure load, respectively.

Figure 4. Reconstructed HRpQCT images showing: **A)** the whole bone, **B)** cortical thickness, and **C)** trabecular thickness at the distal tibia in the nondominant (ND) and dominant (D) arms of a representative tennis player. Tennis players had D-to-ND leg differences in Tt.vBMD and µFE analyses of estimated bone strength, but no measurable D-to-ND leg differences in bone size or microarchitectural properties. The tennis player shown had a 3.5% D-to-ND leg difference in failure load, with 1.3% less Tt.vBMD and 4.1% greater Tt.Ar in the D leg. The participant had no D-to-ND leg difference (0%) in Tb.BV/TV.

Figure 5. Reconstructed HRpQCT images showing: **A)** the whole bone and **B)** cortical thickness at the tibial diaphysis in the nondominant (ND) and dominant (D) legs of the representative tennis player shown in Figure 4. Note the larger area of greater cortical thickness in this particular participant at the anterior and posteromedial cortices. This particular participant had 3.3%, 5.3%, 7.2% and 5.3% greater Tt.Ar, Ct.Ar, Ct.Th, and failure load in their dominant leg compared to nondominant leg, respectively.

SUPPLEMENTAL DIGITAL CONTENT

Suppl_Table_1_distal radius.xlsx: HR-pQCT properties of the distal radius in runners and tennis players

Suppl_Table_2_radial shaft.xlsx: HR-pQCT properties of the radial diaphysis in runners and tennis players

Suppl_Table_3_tibia shaft.xlsx: HR-pQCT properties of the tibial diaphysis in runners and tennis players

Suppl_Table_4_distal tibia.xlsx: HR-pQCT properties of the distal tibia in runners and tennis players
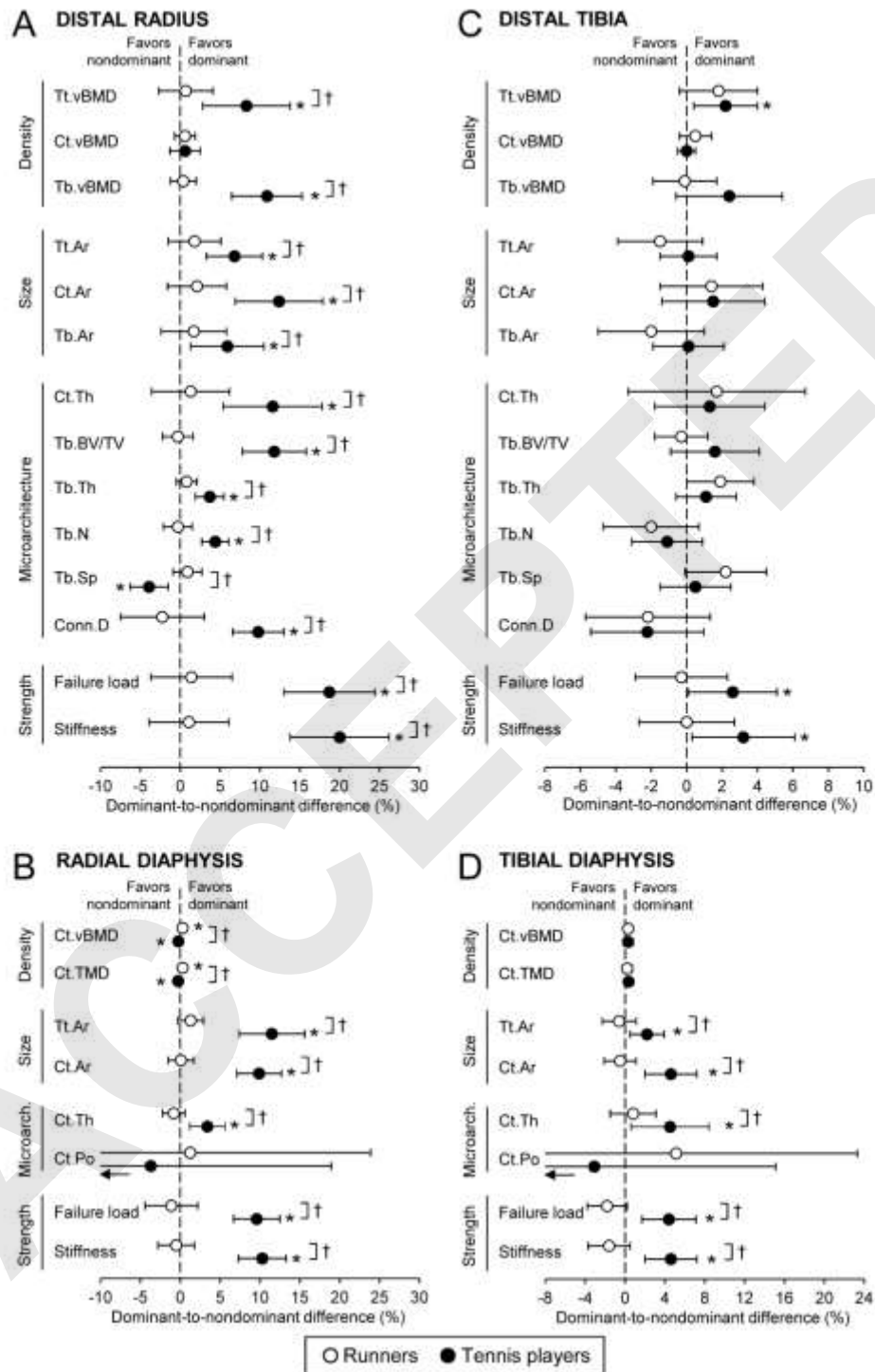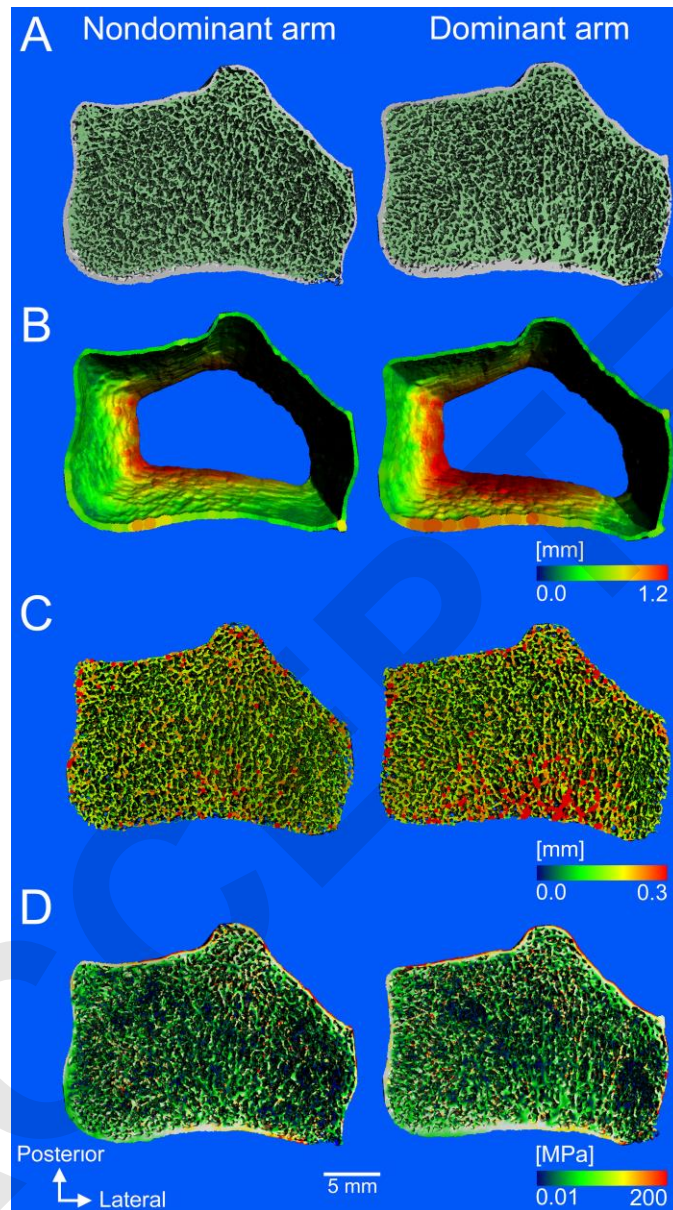
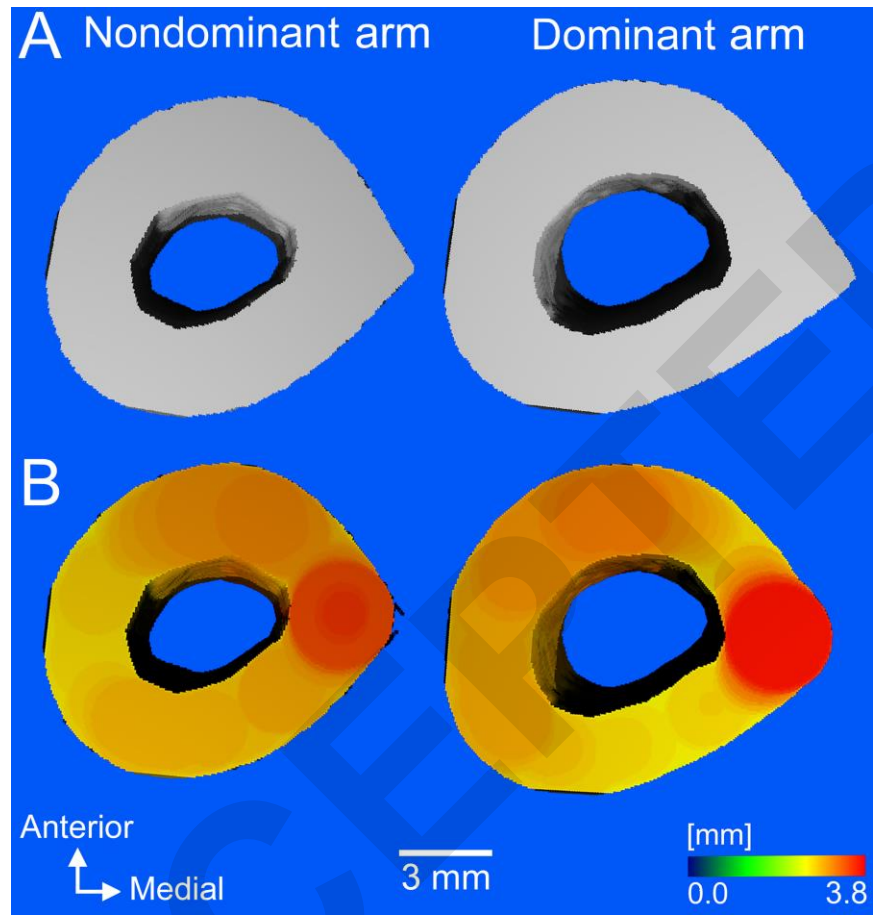**Figure 1**

Figure 2

Figure 3

Figure 4

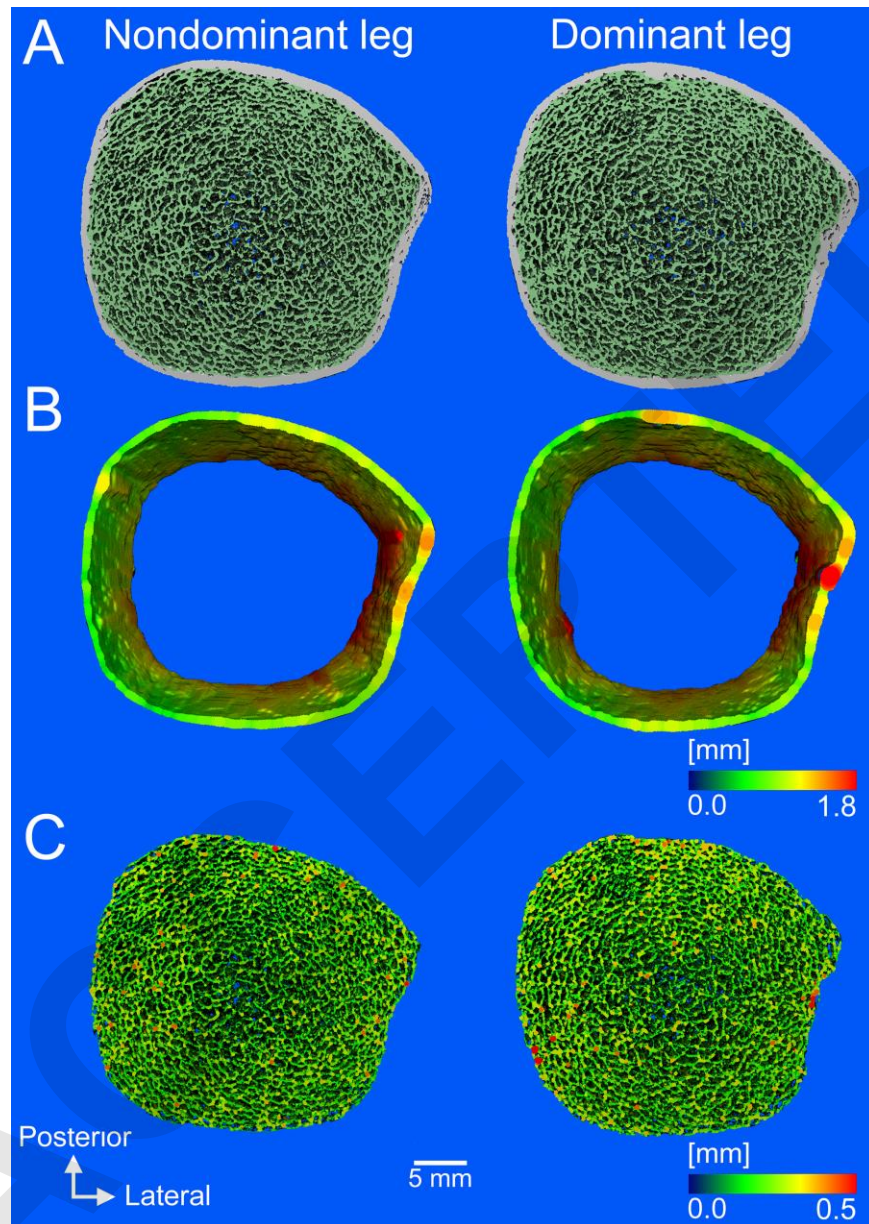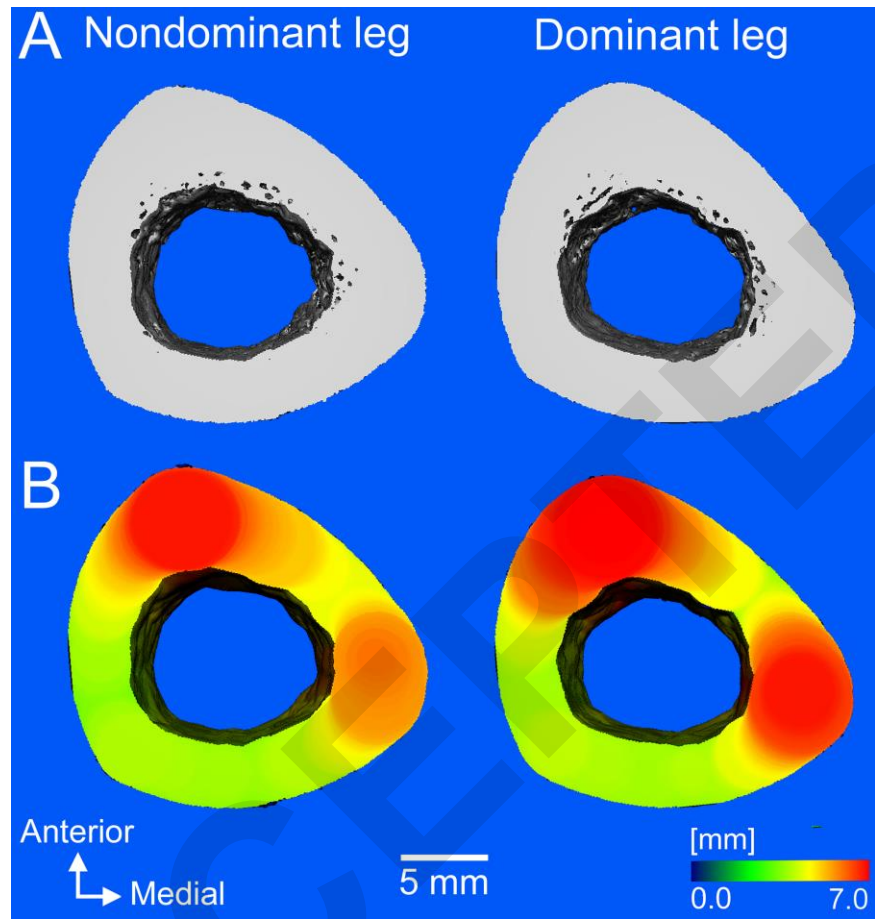**Figure 5**

Supplementary Table 1. HR-pQCT properties of the distal radius in runners and tennis players

	Runners			Tennis players		
	Nondominant[a,b]	Dominant[a]	Abs. diff. (95% CI)[c]	Nondominant[a,b]	Dominant[a]	Abs. diff. (95% CI)[c]
Density						
Tt.vBMD (mg HA/cm^3)	284 ± 45	284 ± 35	0 (-9, 9)	269 ± 36	290 ± 46	22 (7, 37)*
Ct.vBMD (mg HA/cm^3)	860 ± 49	864 ± 38	5 (-7, 16)	863 ± 31	868 ± 31	5 (-11, 20)
Tb.vBMD (mg HA/cm^3)	168 ± 28	168 ± 27	0 (-2, 3)	155 ± 32	172 ± 36	17 (11, 20)*
Size						
Tt.Ar (mm^2)	297 ± 43	303 ± 50	5 (-5, 16)	302 ± 30	322 ± 28	20 (10, 29)*
Ct.Ar (mm^2)	51.0 ± 6.8	51.8 ± 5.6	0.8 (-0.9, 2.6)	50.0 ± 5.5	56.0 ± 6.7	6.0 (3.4, 8.6)*
Tb.Ar (mm^2)	250 ± 42	254 ± 46	4 (-7, 16)	257 ± 32	271 ± 30	14 (4, 24)*
Microarchitecture						
Ct.Th (mm)	0.85 ± 0.14	0.85 ± 0.08	0.00 (-0.04, 0.04)	0.80 ± 0.11	0.89 ± 0.14	0.09 (0.04, 0.14)*
Tb.BV/TV (%)	24.2 ± 4.2	24.1 ± 4.3	0.1 (-0.05, 0.03)	21.8 ± 4.6	24.3 ± 5.2	2.5 (1.7, 3.3)*
Tb.Th (µm)	217 ± 11	219 ± 10	2 (-1, 4)	212 ± 15	220 ± 16	8 (4, 11)*
Tb.N (1/mm)	1.53 ± 0.13	1.53 ± 0.13	0.00 (-0.03, 0.02)	1.61 ± 0.16	1.67 ± 0.19	0.07 (0.04, 0.09)*
Tb.Sp (µm)	599 ± 64	605 ± 66	5 (-6, 17)	581 ± 66	551 ± 56	-24 (-38, -9)*
Conn.D (1/mm^3)	3.86 ± 0.55	3.80 ± 0.77	-0.06 (-0.23, 0.11)	3.72 ± 0.75	4.04 ± 0.70	0.32 (0.10, 0.54)*
Strength						
Failure load (kN)	3.57 ± 0.72	3.61 ± 0.77	0.04 (-0.11, 0.19)	3.17 ± 0.62	3.76 ± 0.83	0.59 (0.41, 0.76)*
Stiffness (kN/mm)	65.5 ± 13.7	66.2 ± 15.0	0.7 (-1.9, 3.3)	57.5 ± 12.5	68.9 ± 16.5	11.4 (7.8, 15.1)*

[a] Data are mean ± SD
[b] Differences in nondominant leg properties between groups were assessed using an unpaired t-test (all $p<0.05$).
[c] Mean absolute differences between dominant and nondominant legs were assessed using single sample t-tests with a population mean of 0. Significance is indicated by: *$p<0.05$.

Supplementary Table 2. HR-pQCT properties of the radial diaphysis in runners and tennis players

	Runners			Tennis players		
	Nondominant[a,b]	Dominant[a]	Abs. diff. (95% CI)[c]	Nondominant[a,b]	Dominant[a]	Abs. diff. (95% CI)[c]
Density						
Ct.vBMD (mg HA/cm^3)	1103 ± 14	1107 ± 17	3 (0, 6)*	1107 ± 15	1104 ± 17	-3 (-6, -0)*
Ct.TMD (mg HA/cm^3)	1108 ± 14	1111 ± 16	3 (1, 5)*	1112 ± 15	1109 ± 14	-3 (-6, -0)*
Size						
Tt.Ar (mm^2)	89.3 ± 11.0	90.5 ± 12.0	1.2 (-0.3, 2.7)	89.2 ± 7.3	99.4 ± 9.6	10.2 (6.6, 13.7)*
Ct.Ar (mm^2)	76.0 ± 6.9	76.1 ± 7.6	0.1 (-1.1, 1.3)	75.4 ± 5.9	82.8 ± 7.6	7.4 (5.3, 9.5)*
Microarchitecture						
Ct.Th (mm)	3.27 ± 0.27	3.24 ± 0.30	0.03 (-0.07, 0.02)	3.19 ± 0.29	3.30 ± 0.34	0.11 (0.04, 0.19)*
Ct.Po (%)	0.43 ± 0.15	0.42 ± 0.25	-0.01 (-0.11, 0.09)	0.42 ± 0.15	0.38 ± 0.12	-0.04 (-0.14, 0.06)
Strength						
Failure load (kN)	4.56 ± 0.42	4.51 ± 0.55	-0.05 (-0.19, 0.10)	4.50 ± 0.39	4.93 ± 0.51	0.43 (0.30, 0.57)*
Stiffness (kN/mm)	76.5 ± 7.3	76.2 ± 8.6	-0.3 (-2.1, 1.4)	75.8 ± 6.3	83.6 ± 8.2	7.8 (5.5, 10.1)*

[a] Data are mean ± SD

[b] Differences in nondominant leg properties between groups were assessed using an unpaired t-test (all $p<0.05$).

[c] Mean absolute differences between dominant and nondominant legs were assessed using single sample t-tests with a population mean of 0. Significance is indicated by: *$p<0.05$.

Supplementary Table 3. HR-pQCT properties of the distal tibia in runners and tennis players

	Runners			Tennis players		
	Nondominant[a,b]	Dominant[a]	Abs. diff. (95% CI)[c]	Nondominant[a,b]	Dominant[a]	Abs. diff. (95% CI)[c]
Density						
Tt.vBMD (mg HA/cm^3)	360 ± 44	366 ± 41	6 (-2, 13)	347 ± 38	354 ± 37	7 (1, 13)*
Ct.vBMD (mg HA/cm^3)	930 ± 38	935 ± 34	5 (-3, 13)	936 ± 22	936 ± 20	0 (-4, 4)
Tb.vBMD (mg HA/cm^3)	219 ± 28	219 ± 30	0 (-4, 4)	212 ± 33	216 ± 30	4 (-2, 10)
Size						
Tt.Ar (mm^2)	635 ± 105^T	625 ± 100	-10 (-25, 5)	706 ± 66^C	707 ± 70	1 (-11, 13)
Ct.Ar (mm^2)	127 ± 19	128 ± 18	1 (-2, 5)	134 ± 18	136 ± 19	2 (-2, 6)
Tb.Ar (mm^2)	513 ± 103	502 ± 97	12 (-27, 4)	577 ± 68	577 ± 67	0 (-12, 13)
Microarchitecture						
Ct.Th (mm)	1.54 ± 0.26	1.55 ± 0.21	0.01 (-0.05, 0.08)	1.51 ± 0.22	1.53 ± 0.22	0.02 (-0.03, 0.06)
Tb.BV/TV (%)	31.5 ± 3.7	31.5 ± 40	0.1 (-0.05, 0.04)	31.0 ± 4.5	31.5 ± 4.1	0.4 (-0.3, 1.2)
Tb.Th (μm)	270 ± 25	276 ± 28	5 (-1, 4)	260 ± 14	263 ± 18	3 (-2, 7)
Tb.N (1/mm)	1.52 ± 0.17	1.49 ± 0.16	-0.03 (-0.08, 0.01)	1.57 ± 0.21	1.55 ± 0.21	-0.02 (-0.05, 0.01)
Tb.Sp (μm)	602 ± 72	616 ± 80	13 (-1, 27)	599 ± 103	601 ± 100	2 (-10, 15)
Conn.D (1/mm^3)	3.05 ± 0.70	2.96 ± 0.60	-0.09 (-0.20, 0.02)	3.40 ± 0.78	3.32 ± 0.77	-0.08 (-0.18, 0.02)
Strength						
Failure load (kN)	11.14 ± 1.80	11.18 ± 1.71	0.00 (-0.23, 0.31)	12.25 ± 1.91	12.52 ± 1.69	0.28 (0.01, 0.56)*
Stiffness (kN/mm)	209.2 ± 35.7	210.5 ± 34.1	1.3 (-3.9, 6.4)	229.4 ± 38.2	235.6 ± 33.5	6.2 (0.2, 12.2)*

[a] Data are mean ± SD

[b] Differences in nondominant leg properties between groups were assessed using an unpaired t-test. Capital letters indicate the non-dominant data differs significantly from controls (C) and tennis players (T) ($p<0.05$)

[c] Mean absolute differences between dominant and nondominant legs were assessed using single sample t-tests with a population mean of 0. Significance is indicated by: *$p<0.05$.

Supplementary Table 4. HR-pQCT properties of the tibial diaphysis in runners and tennis players

	Runners			Tennis players		
	Nondominant[a,b]	Dominant[a]	Abs. diff. (95% CI)[c]	Nondominant[a,b]	Dominant[a]	Abs. diff. (95% CI)[c]
Density						
Ct.vBMD (mg HA/cm^3)	1022 ± 22	1026 ± 23	4 (-1, 9)	1028 ± 22	1031 ± 22	3 (-2, 8)
Ct.TMD (mg HA/cm^3)	1031 ± 22	1035 ± 22	4 (-1, 9)	1036 ± 23	1038 ± 22	2 (-3, 7)
Size						
Tt.Ar (mm^2)	339 ± 45	337 ± 44	-2 (-8, 4)	362 ± 34	370 ± 34	10.2 (6.6, 13.7)*
Ct.Ar (mm^2)	269 ± 37	268 ± 37	-2 (-6, 3)	277 ± 33	289 ± 31	12 (5, 19)*
Microarchitecture						
Ct.Th (mm)	3.27 ± 0.27	3.24 ± 0.30	0.03 (-0.07, 0.02)	6.07 ± 0.86	6.30 ± 0.66	0.23 (0.01, 0.46)*
Ct.Po (%)	0.84 ± 0.44	0.84 ± 0.44	0.00 (-0.12, 0.12)	0.82 ± 0.18	0.78 ± 0.25	-0.04 (-0.18, 0.10)
Strength						
Failure load (kN)	16.04 ± 2.32	15.75 ± 2.28	-0.29 (-0.68, 0.10)	16.23 ± 1.98	16.90 ± 1.76	0.67 (0.24, 1.10)*
Stiffness (kN/mm)	285.0 ± 40.7	280.3 ± 39.1	-4.7 (-10.8, 1.4)	291.6 ± 35.8	304.4 ± 33.3	12.8 (5.1, 20.6)*

[a] Data are mean ± SD

[b] Differences in nondominant leg properties between groups were assessed using an unpaired t-test (all $p>0.05$)

[c] Mean absolute differences between dominant and nondominant legs were assessed using single sample t-tests with a population mean of 0. Significance is indicated by: *$p<0.05$.